Active Rocket Controls (ARC)

Engineering Calculations

Henry Benedictus (Team Lead)

Chyler Bitsoi (CAD lead)

Emilio Huggins (Manufacturing Lead)

AislinnJoy Gacayan (Budget/Fundraising Lead)

Eric Reyes (Communications Lead)

Fall 2025-Spring 2026

Project Sponsor:

Northern Arizona Rocket Club

Bryan Spouse

Faculty Advisor:

Carson Marty Pete

Instructor:

David Willy

Introduction:

This document serves as a comprehensive and updated summary of the necessary calculations performed in designing the subsystems and verifying performance for our rocket. Statements and assumptions will be given, and calculations will be performed with concluding results and the sources used to verify our findings. Critical subsystems evaluated are the connecting screws, fin control angles, specifications for black powder charges and parachute deployment, fuselage and motor centering ring structural analysis, and the performance of the internal control mechanism responsible for fin movement.

Top Level Design Summary:

The Active Rocket Control (ARC) full assembly (Figure 1) consists of two separate subsystems. The first subsystem is the sled assembly (Figure 2), which will hold the sensors, flight computer, and the parachute ejection charge. It connects to the rear fuselage by interlinking the coupler and securing it with screws. The control mechanism (Figure 3) will control the rocket's orientation by actuating the fins and thus changing the angle of attack. It attaches to the rocket by first epoxing the motor rings and aft insert to the motor tube. Then it connects to the rear fuselage by using heat inserts connected to the rings and aft insert and secured with a ¼ in screw.

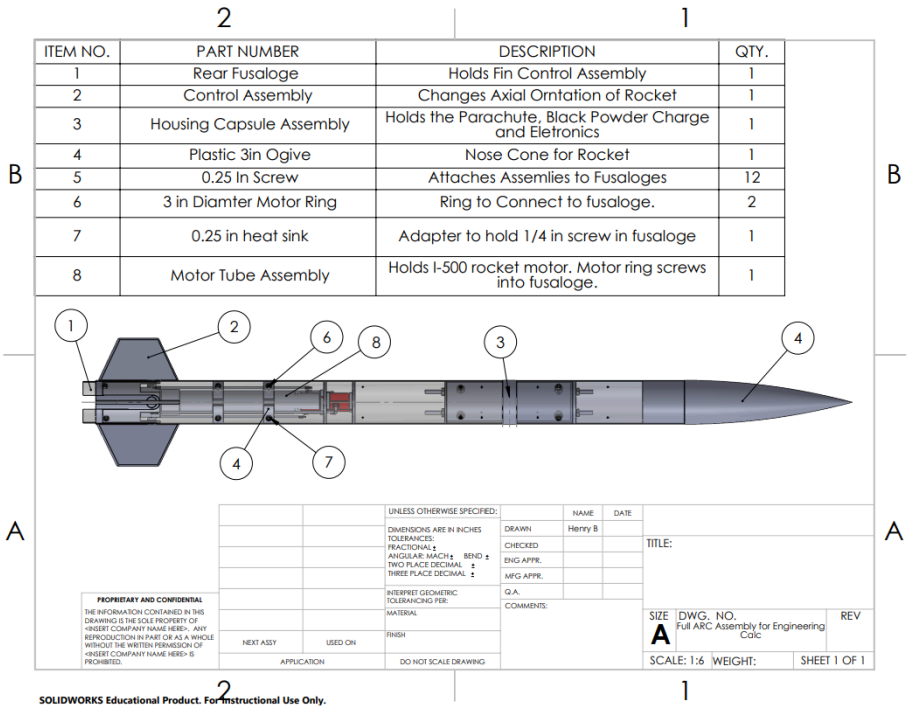

ITEM NO.	PART NUMBER	DESCRIPTION	QTY.
1	Rear Fusaloge	Holds Fin Control Assembly	1
2	Control Assembly	Changes Axial Orntation of Rocket	1
3	Housing Capsule Assembly	Holds the Parachute, Black Powder Charge and Eletronics	1
4	Plastic 3in Ogive	Nose Cone for Rocket	1
5	0.25 In Screw	Attaches Assemlies to Fusaloges	12
6	3 in Diamter Motor Ring	Ring to Connect to fusaloge.	2
7	0.25 in heat sink	Adapter to hold 1/4 in screw in fusaloge	1
8	Motor Tube Assembly	Holds I-500 rocket motor. Motor ring screws into fusaloge.	1

Figure 1: Full ARC Assembly

ITEM NO.	PART NUMBER	DESCRIPTION	QTY.
1	3 in diamter 12 in long tube	Holds Assembly	1
2	Coupler with Switch Band Assebmly	Hods the Sled	1
3	3in diamter bulk plate	Protects the Sensors from Black Powder Blast	1
4	0.2500in with Thread	connects assembly and secures the sled.	8
5	0.25 in 12 in long all thread	Goes through the sled to attach it to bulk plate and plate lid.	2
6	Updated Sled 3in	Holds the sensors.	1
7	Bulk Plate Lid	Secures assembly together	1
8	0.25 in washer	used to seprate nuts with surfaces.	4
9	0.25 in Screw	Secures assembly togther and to the main assembly.	4

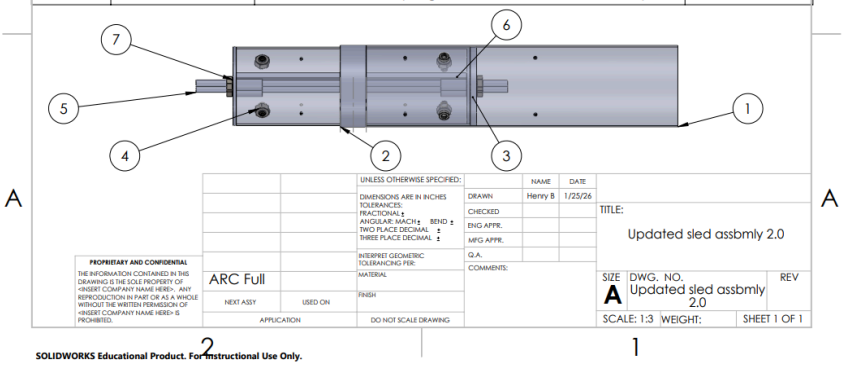

UNLESS OTHERWISE SPECIFIED:
DIMENSIONS ARE IN INCHES
TOLERANCES:
FRACTIONAL ±
ANGULAR: MACH ± BEND ±
TWO PLACE DECIMAL ±
THREE PLACE DECIMAL ±
INTERPRET GEOMETRIC TOLERANCING PER:
MATERIAL
FINISH
DO NOT SCALE DRAWING

	NAME	DATE
DRAWN	Henry B	1/25/26
CHECKED		
ENG APPR.		
MFG APPR.		
Q.A.		
COMMENTS:		

ARC Full
NEXT ASSY | USED ON
APPLICATION

TITLE: Updated sled assbmly 2.0
SIZE A | DWG. NO. Updated sled assbmly 2.0 | REV
SCALE: 1:3 | WEIGHT: | SHEET 1 OF 1

Figure 2: Sled Sub Assembly

ITEM NO.	PART NUMBER	DESCRIPTION	QTY.
1	Aft insert	Used to both hold part of the motor tube and control mech.	1
2	Fin	Controls the orentation of the rocket.	4
3	Lower fin arm	Connects the fins to the push rods.	4
4	M3 Tierod	Servos to control mechanism.	8
5	Servo holder pt 4	Holds the servos in the assembly	1
6	servo horn	Connects the push rods to the servos.	4
7	servo.solid round pt2	Holds part of the servos	4
8	push 11 inc	11 inch push rod to connect fins to servos.	2
9	13 inch push rod	11 inch push rod to connect fins to servos.	2

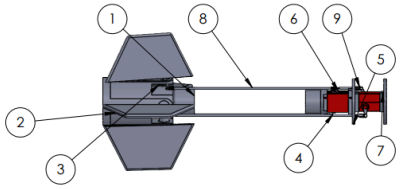

UNLESS OTHERWISE SPECIFIED:
DIMENSIONS ARE IN INCHES
TOLERANCES:
FRACTIONAL ±
ANGULAR: MACH ± BEND ±
TWO PLACE DECIMAL ±
THREE PLACE DECIMAL ±
INTERPRET GEOMETRIC TOLERANCING PER:
MATERIAL
FINISH
DO NOT SCALE DRAWING

	NAME	DATE
DRAWN	Henry B	1/25/26
CHECKED		
ENG APPR.		
MFG APPR.		
Q.A.		
COMMENTS:		

Full ARC
NEXT ASSY | USED ON
APPLICATION

TITLE: Control Mech Assembly
SIZE A | DWG. NO. Control Mech Assembly | REV
SCALE: 1:8 | WEIGHT: | SHEET 1 OF 1

Figure 3: Control Mechanism Assembly

Quality Function Diagram

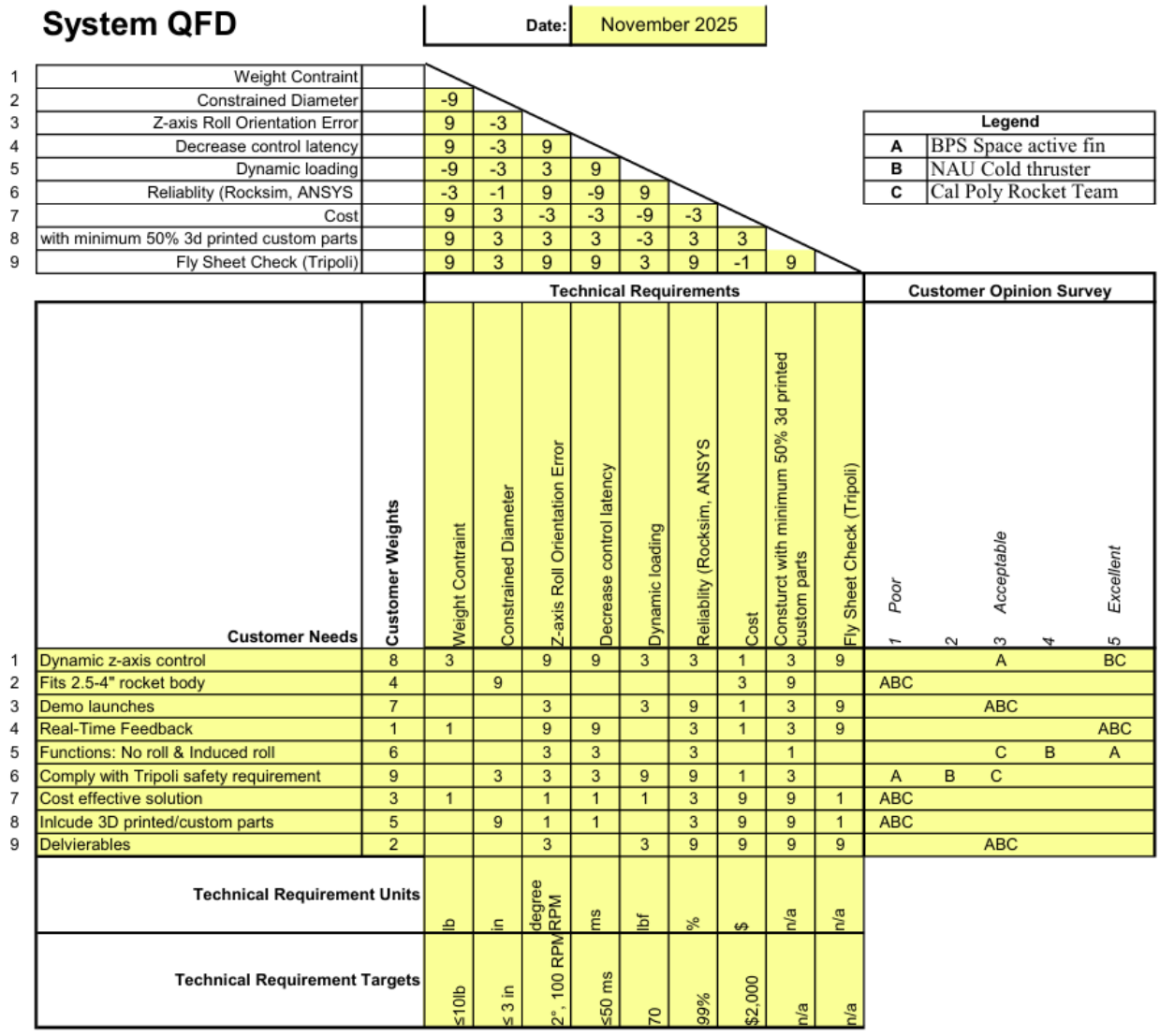

System QFD

Date: November 2025

1	Weight Contraint								
2	Constrained Diameter		-9						
3	Z-axis Roll Orientation Error		9	-3					
4	Decrease control latency		9	-3	9				
5	Dynamic loading		-9	-3	3	9			
6	Reliablity (Rocksim, ANSYS		-3	-1	9	-9	9		
7	Cost		9	3	-3	-3	-9	-3	
8	with minimum 50% 3d printed custom parts		9	3	3	3	-3	3	3
9	Fly Sheet Check (Tripoli)		9	3	9	9	3	9	-1

Legend	
A	BPS Space active fin
B	NAU Cold thruster
C	Cal Poly Rocket Team

			Technical Requirements								Customer Opinion Survey				
	Customer Needs	Customer Weights	Weight Contraint	Constrained Diameter	Z-axis Roll Orientation Error	Decrease control latency	Dynamic loading	Reliablity (Rocksim, ANSYS	Cost	Consturct with minimum 50% 3d printed custom parts	Fly Sheet Check (Tripoli)	1 Poor	2	3 Acceptable	4	5 Excellent
1	Dynamic z-axis control	8	3		9	9	3	3	1	3	9			A		BC
2	Fits 2.5-4" rocket body	4		9					3	9		ABC				
3	Demo launches	7			3		3	9	1	3	9			ABC		
4	Real-Time Feedback	1	1		9	9		3	1	3	9					ABC
5	Functions: No roll & Induced roll	6			3	3		3		1				C	B	A
6	Comply with Tripoli safety requirement	9		3	3	3	9	9	1	3		A	B	C		
7	Cost effective solution	3	1		1	1	1	3	9	9	1	ABC				
8	Inlcude 3D printed/custom parts	5		9	1	1		3	9	9	1	ABC				
9	Delvierables	2			3		3	9	9	9	9			ABC		
	Technical Requirement Units		lb	in	degree RPM	ms	lbf	%	$	n/a	n/a					
	Technical Requirement Targets		≤10lb	≤ 3 in	2°, 100 RPM	≤50 ms	70	99%	$2,000	n/a	n/a					

Figure 4: ARC QFD

Engineering Requirements

Dynamic Z-Axis Control: The system must control the rocket about the z-axis, which includes mating stability during flight and trajectory control.

Fits System into a 2.5-4 in Diameter Body: All components must fit inside a minimum of 2.5 inches and a maximum of 4in rocket body, which includes motor, motor mounts, avionics bay, and sensors.

Demo Launch: The system must demonstrate functionality in two test phases: a basic flight demonstration by January 2026 and a fully integrated active control demonstration during a Tripoli live

test by March 2026.

Sensor Feedback: The control system must be integrated using an Arduino-based control, and the sensor must be able to record flight data.

Function of No Roll and Induced Roll: The dynamic control system must be able to provide two primary functions. One that is an induced roll for a specified amount of time and a stabilized function that induces no roll.

Comply and Follow Tripoli Safety Standards: The design must adhere to Tripoli Rocketry Association safety regulations and operational standards for high-powered rocketry. Including a preflight sheet and RockSim validation before launch.

Find the Most Cost-Effective Solution: The team must explore 3 different methods of active control systems and perform a cost analysis to meet the maximum $2000 budget.

Include 3D printed Components/Parts: At least 50% of the constructed control system must be manufactured via 3D printing methods.

Deliverables: The project must include all final deliverables, such as flight test data, design documentation, and system verification reports, as outlined in the sponsor agreement.

Customer Requirements

Weight Constraint: The total rocket system must not exceed 10lb to ensure flight stability and compatibility with flight vehicles.

Constrained Diameter: All systems must fit into a 2.5 in - 4 in rocket tube diameter.

Z-Axis Roll Control Error: The roll orientation error must remain below 2° during active control.

Induce Roll Rate: System must induce and damp roll to 100 RPM within 2 s and then stop rotation.

Control Latency: Control loop latency must be under 50 ms to ensure reliable control over the rocket control system.

Dynamic loading capacity: The system must handle aerodynamic and inertial loading of at least 70 lbf.

Reliability: The control system must achieve at least 99% operational reliability during test launches.

Cost Constraint: Total system cost should not exceed $2,000.

Custom Part Integration: At least 50% of system components must be custom-fabricated or 3D printed.

Summary of Standards, Codes, and Regulations:

Tripoli Rocketry Association Unified Safety Code [1]

7-1.1 Construction; rockets shall be built using lightweight materials, such as paper, wood, plastic, rubber, or, when necessary, ductile lightweight metals, and construction techniques that are suitable for the planned flight.

7-1.2 Stability; the flier shall document the location of the center of pressure and be able to demonstrate the center of gravity.

7-1.3 Every rocket shall include a recovery system sufficient to allow the rocket to land at a safe velocity.

7-1.4 The thrust-to-weight ratio of a rocket typically should be at least 5:1. However, the RSO may approve a thrust-to-weight as low as 3:1 ratio. Initial thrust-to-weight ratios lower than 3:1 may only be authorized by an RSO if an active stability system is included.

11-1 A rocket shall be launched only if it has a recovery system designed to return all parts of the rocket to the ground safely and at a landing speed not to exceed 35 feet/second (11 meters/second). Higher landing speeds may be approved by the BoD before the flight.

Equations

The following summary of equations specifically complies with safety standards outlined in the Tripoli Rocketry Unified Safety Code.

Structure and Stability

- Fastener shear and deflection: 1 - 4
- Axial Stress and Buckling: 27 - 32
- Bending and Combined Stress: 33 - 39
- Centering Ring Compression and Strain: 40 - 43

Recovery Regulations and Descent Rate

- Ejection Charge: 19 - 21
- Parachute Sizing: 22 - 26

Summary of Equations and Solutions:

Shear Force Analysis on Connecting Screws - Henry Benedictus

The Active Rocket Control system will have a modular motor ring to easily take the aft end of the rocket and its associated components out for ease of maintenance and assembly. The motor rings have a hole in

the middle for the motor to be in, and then on the outer edges, there are 4 screw holes on each ring (3 rings in total). On the rocket fuselage, there are associated holes in which the screw will go to connect to the motor ring. These 12 screws will then hold the entire motor system to the fuselage. The purpose of this analysis is to find the shear stress of the screws to choose a correct diameter and material property.

Assumptions

The I500 rocket motor that was chosen for launch produces a maximum force of 640 N according to its manufacturer, AeroTech [2]. Since all three motor rings are connected to the motor itself, it is assumed that each of the top screws is undergoing 640 N, with a factor of safety (FS) of 2. The tables for screw size and material properties are found within [3] . Equations 1 and 2 will be used to find the shear stress that the screw undergoes and the maximum shear that it can withstand. Equations 3 and 4 are used to find the maximum deflection of the screw to compare it to the FEA model.

$$\tau = \frac{\nu}{A_s} (1) \qquad \tau_{Allow} = \frac{\tau_{Shear}}{F.S} (2)$$

$$\delta_{max} = \frac{PL^3}{3EI} (3) \qquad I = \frac{\pi r^4}{16} (4)$$

Shear Force (ν)	1280 N
Radius (r)	0.125in
Force (P)	1280 N
Length (L)	0.748 in

Table 1: Screw Shear Mathematical Modeling Units

Besides using mathematical modeling to determine the screws that will need to be used, the built-in Finite Element Analysis (FEA) stress modeling within SolidWorks is used. To perform this test, the fuselage that is planned to be used for the system is modified within SolidWorks and will have fiberglass as its assigned material. For the motor ring, its material will be Polylactic Acid (PLA) since, at the moment, those parts will be 3D printed. The ¼ in screw that will be used for the simulation was modeled by Carlos Lopez and open-sourced from Grab CAD [4]. The material of the screw will be based on readily available ¼ in screws that can be bought commercially (Walmart, Home Depot, Lowes, etc). The screw that is used is a hex screw that is readily available at Home Depot. A ¼ in screw and a larger screw adapter for ¼ are readily available if need be.

Material Properties

Within Table 10, the material properties for each material that will be used for this simulation are presented in standard units. Each property is entered in as a custom material within SolidWorks since it does not have these specific materials prelisted.

	PLA	G12 Fiber Glass	A574 Alloy Steel
Elastic Modulus (psi)	290075	$12.3282 * 10^6$	180000

Poisson's Ratio	0.3	0.23	0.3
Shear Modulus (psi) (τ_{shear})	350000	$5.22136 * 10^6$	72000
Density (lb/in^3)	0.047	0.09375	0.284
Tensile Strength (psi)	5801.5	$297.327 * 10^3$	180000
Citation	[5]	[6]	[7]

Table 2: Material Properties for Screw Analysis

SolidWorks FEA

After entering all the associated values into the SolidWorks Material, a 1280 N distributed force was applied to one of the rings. The fuselage had a static boundary condition applied to it in all directions. However, when testing this within SolidWorks FEA, it couldn't detect the connection between the bolts and the inner motor ring.

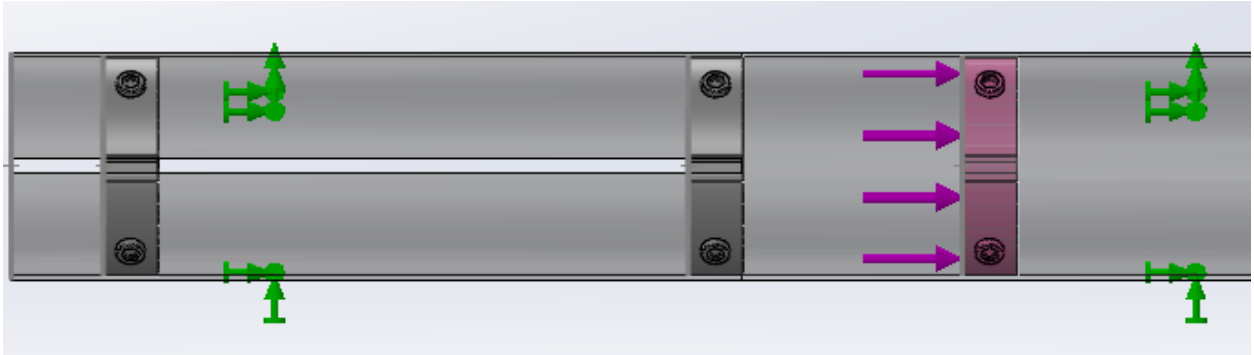

Figure 5: Applied Boundary Conditions of Motor Rings and Bolts

Since the initial test didn't work, a bending force test was performed for a single bolt, undergoing a force of 1260 N along the entire mid-length of the bolt. A displacement boundary condition was applied to the head of the bolt since it will not be undergoing any noticeable forces. This can be seen within Figure 6 with the generated mesh with a fineness between fine and medium.

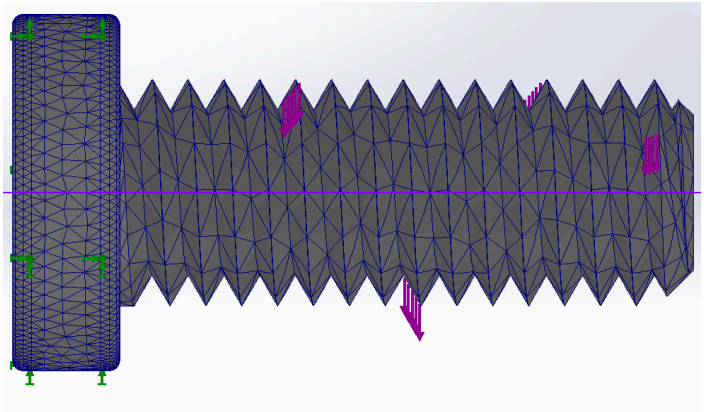

Figure 6: Applied Boundary Conditions and Mesh of Screw

After the boundary conditions were applied and the mesh created, the simulation ran. It took approximately 5 minutes to complete. Once complete, it generated the displacement (Figure 7), Strain (Figure 8), and Stress (Figure 9) experienced by the screw. It experienced a maximum displacement of 1.386 mm (0.055in), maximum stress of 3.170E4 N/m^2, and maximum strain of 5.195E-5. Based on the simulation, the chosen screws are strong enough to withstand double the force they would be estimated to be undergoing.

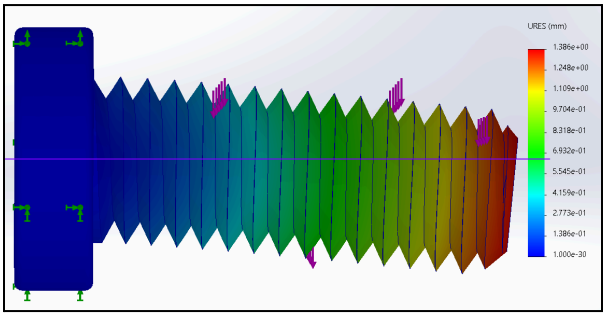

Figure 7: Displacement of Screw

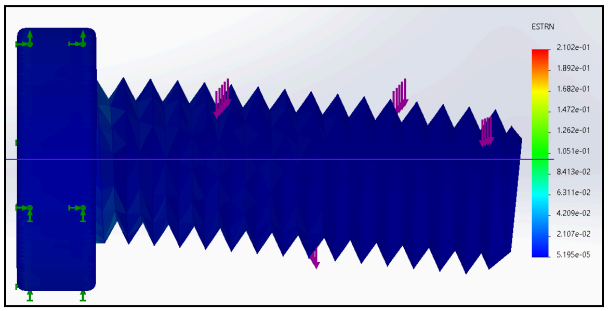

Figure 8: Strain of Screw

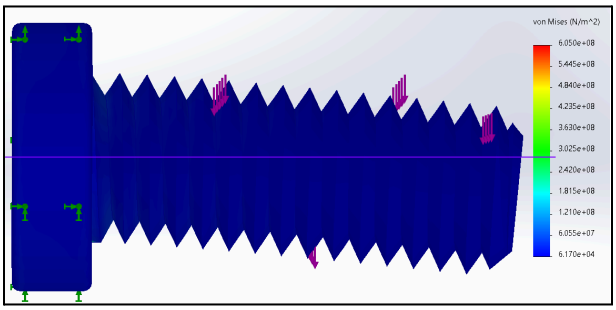

Figure 9: Stress of the Screw

Mathematical Calculations

First, finding the Shear Force of the screw, equations 1 and 2 were used. Based on the results, the estimated shear force experienced by the bolt is over 6 times the allowed shear stress of the bolt.

$$\tau = \frac{v}{A_s} = \frac{1280N}{(1/4in)/25.4\ (mm/in)} = 40.5MPa \qquad \tau_{Allow} = \frac{72000psi\ */145\ (MPa/psi)}{2} = 248\ MPa$$

To compare the results from the FEA simulations, equation 3 was used, which simulates a cantilever beam with a load at the end of the beam. After the calculation was done, it had an absolute error of 1.4%. This value could increase by not

$$\delta_{max} = \frac{PL^3}{3EI} = \frac{1260N*0.225\ (lbs/N)\ *\ (0.748in*39.37\ (m/in))^3}{3*180E3psi/(145\ (MPa/psi))*7.67E{-}4in^4*(4.16*10^{-7}in^4/m^4)} = 0.0014m\ =\ 1.4mm$$

Results

The results from the FEA and Mathematical Modeling show that a singular screw chosen from Home Depot can withstand the entire force exerted by the rocket. This means that the entirety of the 12 screws is plenty strong enough to secure the rocket to the fuselage, especially during launch, where the maximum force appears. It can also be concluded that a screw that is slightly smaller in diameter or weaker material could also be used if need be. The tests conducted also prove that attaching the motor and motor rings to the fuselage through a screw is feasible.

Fin Control Angle - Henry Benedictus

The methodology of control of the ARC is by alternating the aft fins in either positive or negative degrees to induce or control a fin. Changing the angle of attack of the fins causes a force on the center of pressure of the fin which adds a moment around the z-axis to induce or prevent a roll.

Center of Pressure of Fins

A trapezoid shape was determined to be the best shape to be implemented since it is structurally robust and flutter resistant [8]. The group then designed the fin to be used based on the trapezoid fin used of the Hi-Tech rocket that was used for prototypes 1 and 2.

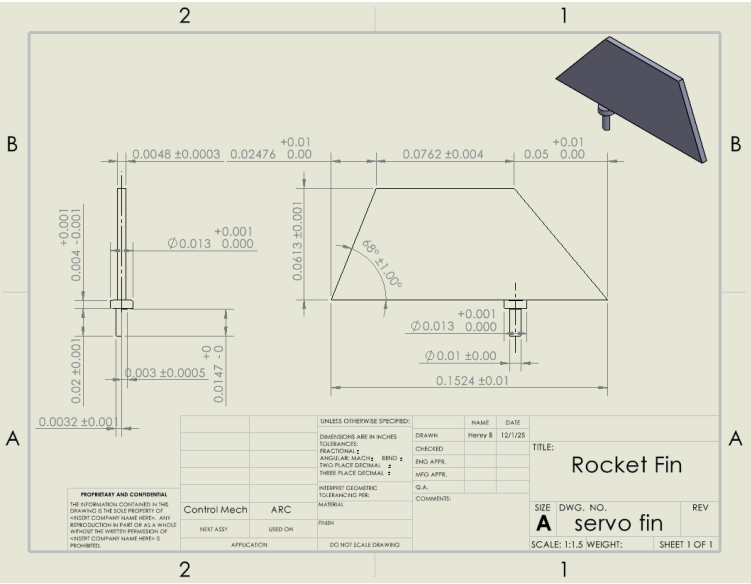

Figure 10: Rocket Fin Drawing (m)

Equations 5 and 6 are used to find the center of pressure along the x and y coordinates of the fins. Figure 11 is used to find the corresponding dimensions used to find the center of pressure [8].

$$\bar{x} = \frac{x_t}{3}\left(\frac{c_r+2c_t}{c_r+c_t}\right) + \frac{1}{6}\left[c_r + c_t - \left(\frac{c_r c_t}{c_r+c_t}\right)\right] \quad (5)$$

$$\bar{y} = \frac{s}{3}\left(\frac{c_r+2c_t}{c_r+c_t}\right) \quad (6)$$

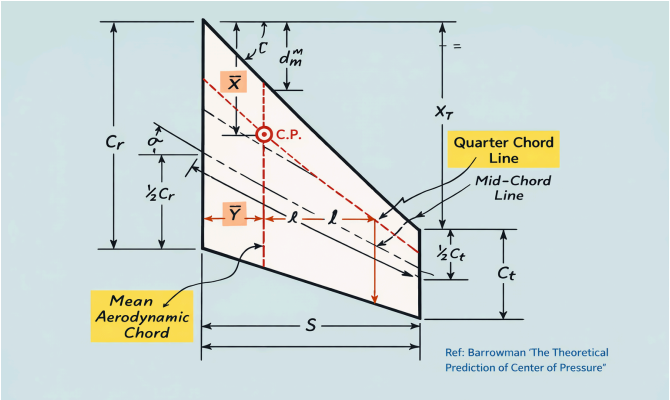

Figure 11: Location of Fin Center of Pressure [8]

Distance Between Fin Root and Fin Tip (x_t or x_r)	Fin Root Cord (c_r)	Fin Tip Cord (c_t)	Exposed Fin Semispan Exposed at Root (s)
0.05162	0.1524	0.0762	0.0613

Table 3: Center of Pressure Location Values (m) [9]

$$\bar{x} = \frac{0.05162}{3}\left(\frac{0.1524+(2)0.0762}{0.1524+0.0762}\right) + \frac{1}{6}\left(0.1524 + 0.0762 - \left(\frac{0.1524*0.0762}{0.1524+0.0762}\right)\right) = 0.05256m$$

$$\bar{y} = \frac{0.0613}{3}\left(\frac{0.1524+0.0762(2)}{0.1524+0.0762}\right) = 0.02724m$$

Normal Force Coefficient

The Normal Force Coefficient ($C_{N\alpha}$) is the coefficient of force perpendicular to the object, dependent on the air flow along the object [8]. $C_{N\alpha}$ is notated by equation 7 [8]. The locations of each variable can be found within Table 3.

$$(C_{N\alpha}) = \left(1 + \frac{fR}{s+R}\right)\left[\frac{4N\left(\frac{s}{d}\right)^2}{1+\sqrt{1+\left(\frac{2l}{c_r+c_t}\right)^2}}\right] \quad (7)$$

$$l = \frac{s}{cos\theta} \quad (8)$$

$$\theta = arctan\left[\frac{1}{s}\left(x_r + \frac{1}{2}(c_t - c_r)\right)\right] \quad (9)$$

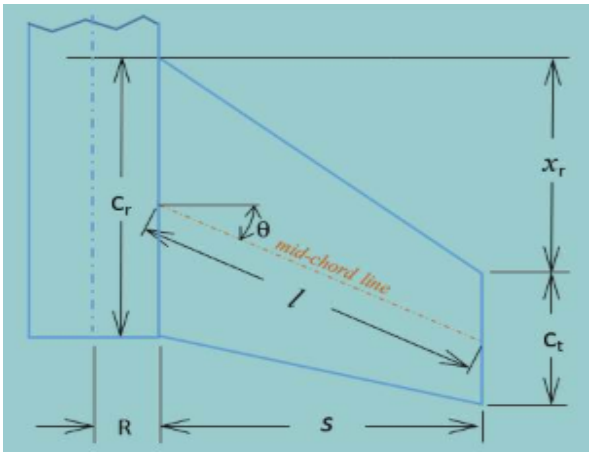

Figure 12: Normal Force Coefficient Locations [8]

$$\theta = arctan[\frac{1}{0.0613}(0.05162 + \frac{1}{2}(0.0762 - 0.1524) = 0.217$$

$$l = \frac{0.0613}{cos 0.127} = 0.0618m$$

$$(C_{N\alpha}) = (1 + \frac{1*0.039624}{0.0613+0.039624})\frac{4*4*(\frac{0.0613}{0.08128})^2}{1+\sqrt{1+(\frac{2*0.0618}{0.0762+0.1524})^2}} = 5.93$$

Normal Force

The Normal Force (F_N) is the force that acts on the center of pressure of an object due to the external fluid acting upon the object [9].

$$N_F = F_\alpha = qA_{Fin}\alpha(C_{N\alpha}) \quad [8] \tag{10}$$

$$q = \frac{1}{2}\rho V^2 \quad [8] \tag{11}$$

$$A = \frac{1}{2}(c_t + c_r)S \quad [10] \tag{12}$$

$dynamic\ pressure\ (q)\ (N/m^2)$	$Density\ (\rho) = 0.91\ (kg/m^3)\ (@3000ft)$
$Area\ of\ Trapazoid\ (A) =\ (m^2)$	$Velocity\ (V) =\ 200\ (m/s)$
$\alpha = Effective\ angle\ of\ attack\ (Radians)$	$I = Moment\ of\ Inertia\ (kg * m^2)$

Table 5: Normal Force Units

$$q = \frac{1}{2}(0.91)(200) = 91\ N/m^2$$

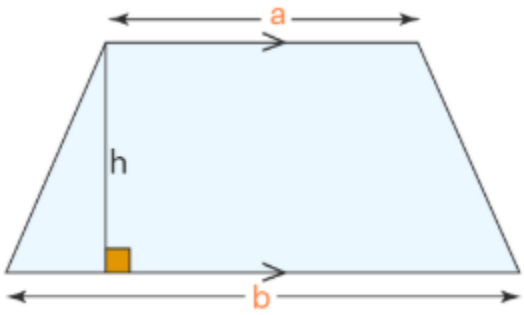

Figure 13: Area of a Trapezoid [10]

$$A = \frac{1}{2}(0.0762 * 0.1524)\, 0.0613 = 3.59 * 10^{-4} m^2$$

The four distinct forces acting on the center of pressure of the fin are found using the normal force equation (10). Figure 14 shows the force directions of each of these forces. Equation 13 is used to find the total moment force (F_{α}). It is multiplied by four since all four fins are undergoing the moment.

$$M_{\alpha} = 4 * F_N * \bar{y} \quad [8] \tag{13}$$

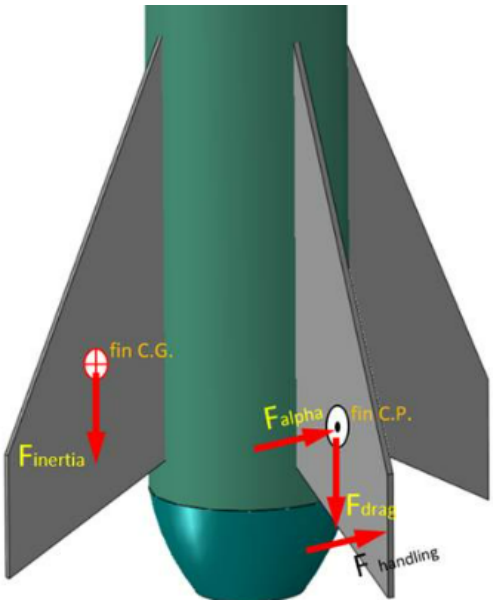

Figure 14: Forces Experienced by Fins [8]

Roll Rate

The roll rate is dependent on the Total Moment of Inertia (I_{Total}) of the rocket, which is comprised of the Moment of Inertia of the Cone (I_{Cone}) and of the body itself (I_{Body}). I_{Body} uses only one radius because the thickness of the rocket is small enough that it doesn't impact the results.

$$I_{Total} = I_{Cone} + I_{Body} \quad (14)$$

$$I_{Body} = m_{body} r^2 \quad [11] \quad (15)$$

$$I_{Nose} = \frac{3}{10} m_{nose} r^2 \quad [12] \quad (16)$$

$Mass\ of\ Nose\ Cone\ (m_{cone}) = 0.1333\ kg$	$Mass\ of\ Rocket\ (m_{body}) = 0.78kg$
$Radius\ of\ Nose\ Cone = 0.039624m$	$Radius\ of\ Rocket = 0.039624m$

Table 6: Mass and Radius of Rocket

$$I_{Body} = 0.78 * 0.039624^2 = 0.00122\ kg * m^2$$
$$I_{nose} = \frac{3}{10} 0.1333 * 0.039624 = 0.00158\ kg * m^2$$
$$I_{Total} = 0.00122 + 0.00158 = 0.0028\ kg * m^2$$

Once the Normal Force and the Total Moment of Inertia are found, the angular velocity (ω) can be found using the two equations. Using angular velocity, the final rotation speed in RPM (n) is found.

$$\omega = \frac{M_\alpha}{I_{Total}} \quad [13] \quad (17)$$

$$n = \frac{\omega}{2\pi} \quad [13] \quad (18)$$

Finding Optimal Angle of Attack

Using the equations and values previously found, the optimal angle of attack (α) can be found.

$$100\ RPM = \frac{\omega}{2\pi} \rightarrow 100\ RPM * 2\pi = \omega \rightarrow \omega = 10.47\ rad/s$$

$$10.47\ rad/s = \frac{M_\alpha}{0.0028\ kg*m^2} \rightarrow M_\alpha = 10.47\ rad/s * 0.0028\ kg * m^2 \rightarrow M_\alpha = 0.02932\ \frac{kg*m^2}{s}$$

$$0.02932\ \frac{kg*m^2}{s} = 4 * F_N * 0.02724m \rightarrow 0.02932\ \frac{kg*m^2}{s} / (4 * 0.02724m) \rightarrow F_N = 0.26909N$$

$$0.2690N = 91\ N/m^2 * 3.59 * 10^{-4} m^2 * 5.93 * \alpha \rightarrow 0.2690N / (91\ N/m^2 * 3.59 * 10^{-4} m^2 * 5.93)$$

$$\alpha = 0.15\,rad = 8.6\,degrees$$

Concluding Remarks

From the information provided, an angle of attack of 8.6 degrees is reasonable to get the rocket to 100 RPMs. However, 8.6 degrees of freedom is not ideal since an increase in the angle of attack. In the future, a team member will develop a MATLAB script to simulate the ideal time to spin the rocket and at what degree from the data provided by RockSim, once it is finalized with all the weights and dimensions of every component of the rocket. Along with the rocksim data, the team plans to do a second test launch that will test a 3-fin rocket with each fin angled at 2 degrees in order to prove the equations stated above.

Ejection Charge and Parachute Analysis - AislinnJoy Gacayan

While conducting the project, it is vital that we ensure all safety regulations are met and that our rocket and systems are maintained following all testing. This analysis answers the following questions: How much ejection charge is required to deploy the parachute? What are the minimum dimensions required for the parachute to safely deliver the rocket back to ground?

Assumptions and variables

In order to answer the problem questions, various assumptions and variables are used to perform the necessary calculations. For the ejection charge calculation, the properties of the black ejection powder, the rocket dimensions, and additional environmental information are needed. The black powder utilized is FFFFg (4Fg), which is the smallest grain type [14]. The gas properties associated with the powder, once lit, that are needed are the combustion gas constant (R) and combustion gas temperature. These variables have values of R = 22.16 ft-lbf/lbm*R and T = 3307 degrees R [15]. The inner diameter of the rocket that the parachute will sit in has a value of 3 inches. The capsule section that will contain the required pressure has a length of about 6 inches. According to a representative from Apogee Components, a good range for the desired pressure within this section for model rockets is 10 -15 psi. For this assessment, a value of 10 psi will be used [14].

For the parachute analysis, environmental factors and rocket performance data gathered from Rocksim testing are used. The rocket launches will be held in Wickenburg, AZ, which has an elevation of around 2,202 feet above sea level (671.17 m). For this analysis, based on the Rocksim results, an additional 4,000 ft (1219.2 m) will be considered for the maximum altitude reached. The launch will be held in March, so the analysis will need to account for colder temperatures. For now, a temperature of 40 degrees Fahrenheit (277.594 K) will be used with a standard temperature lapse rate of 0.0065 K/m. For standard atmospheric pressure, a value of 30 inHg (101592 Pa) will be used [c]. For acceleration due to gravity, 9.81 m/s² will be used. Additionally, for R_{air} the universal gas constant value of 287 J/kg*K is used. Utilizing data from the Rocksim test, the total mass of the rocket with an empty motor is around 1,254.85 g. The coefficient of drag (C_d) is 0.75. According to Tripoli's safety code, the descent velocity cannot exceed 35 ft/s (10.67 m/s²) [1]. Therefore, in order to determine a minimum size of parachute, this analysis will utilize a landing speed of 34 ft/s (10.36 m/s²). Additionally, it will be calculated for a landing speed of 15 ft/s (4.57 m/s²), for a safer buffer and comparison.

Calculations

Black Powder Ejection Charge

The first equation that needs to be determined is the volume of the capsule where the pressure will be. That can be determined by multiplying the area of the section and multiplying it by the length, as seen in equation 19.

$$V = \frac{\pi}{4} * D^2 * L \tag{19}$$

To find the mass of the black powder needed, the ideal gas law can be used. That can be determined by multiplying the desired pressure by the volume obtained from equation 19, and then dividing it by the product of the combustion gas constant and combustion gas temperature. A unit conversion of 1 lbm = 454 grams and 12 in = 1 ft will be used to ensure the final value is in grams.

$$m = \frac{PV}{RT} \tag{20}$$

To determine the force that will result from the amount of black powder used, the desired pressure can be multiplied by the area.

$$F = P * \frac{\pi}{4} * D^2 \tag{21}$$

Parachute Sizing

Before the area can be determined, environmental factors such as temperature, pressure, and air density must be taken into account. Equations 22 - 24 will be used to determine the standard temperature, pressure, and density for conditions during the launch in Wickenburg, Az.

$$T = T_0 - \alpha * h \tag{22}$$

$$P = P_0\left(\frac{T}{T_0}\right)^{\frac{gM}{R*\alpha}} \tag{23}$$

$$\rho = \frac{P}{RT} \tag{24}$$

To determine the area needed for the given factors, this can be found by multiplying 2 by the acceleration due to gravity and the mass of the rocket with an empty motor, and dividing it by the density at the given elevation multiplied by the coefficient of drag and the descent velocity squared. [17]

$$S = \frac{2*g*m}{\rho*C_d*V^2} \tag{25}$$

For a parachute that is round, the diameter can then be determined using the following relation.

$$D = \frac{4*S}{\pi} \tag{26}$$

Results and Discussion

Black Powder Ejection Charge

Using equation 19, the volume of the pressurized section is 42.4 in³. From equation 20, the minimum amount of black powder needed for an ejection pressure of 10 psi is 0.22 grams. From equation 21, the ejection force for the given variables is 71 lbf.

According to Apogee components' information on ejection charges, for a single-use motor that is around 38 mm, the ejection charge is normally around 1.3 grams of black powder [18]. However, for the friction-fitted nose cone we will utilize, the ejection force that will result from the amount of black powder use is more than enough. The force simply needs to be larger than the force of friction from the nose cone. This can also be tested on the ground to validate the calculations. Using a more conservative amount that meets the desired objectives will allow for better resource allocation.

Parachute Sizing

Using equations 22-24, the following values were found:

T = 265.307 K

P = 80063.99 Pa

ρ = 1.051 kg/m^3 = 1051 g/m^3

From equation 25, the minimum area required in order to meet a descent velocity of 34 ft/s (10.36 m/s²) is 0.291 m². The area resulting from a desired landing speed of 15 ft/s (4.57 m/s²) is 1.496 m². The associated diameters are 0.37 and 1.90 m, respectively. This is important as the larger the parachute is, the harder it will be to fit inside the fuselage with the other components, such as the housing module for electronics. Having the room to be a little more conservative with the parachute sizing while also maintaining safety standards and ensuring the structure and parts of our rocket are well maintained during testing will be beneficial when improving the design.

Concluding Remarks

The analysis provided within this report is vital to safety and maintenance considerations for the active rocket controls capstone project. Using mathematical relations and consideration of environmental conditions as well as the Tripoli launching safety code, values were found for both the amount of black powder needed for an effective ejection charge as well as the recommended parachute size. The analysis provided results that will allow the group to be conservative with it's resource management as smaller amounts were calculated for and found to still be effective.

Fuselage Structural Analysis - Emilio Huggins

For final construction, dimensions were minimally changed, and materials were updated from previous prototype construction from 3D-printed PLA to a filament-wound G12 fiberglass tube. Checking for axial compression, ascent will be powered with an H100 motor with a max thrust of 613 N.

Body Dimensions:

$D_i = 3.000\,in = 0.0762\,m$, $D_o = 3.120\,in = 0.079248\,m$,

$t = (D_o - D_i)/2 = 0.060\,in = 1.524\,m$

Cross-sectional area:

$$A_c = \frac{\pi}{4}\left(D_o^2 - D_i^2\right) = 3.72 * 10^{-4}\,m^2 \quad (27)$$

Axial Compressive stress (thrust):

$$\sigma = \frac{F_{max}}{A_c} = \frac{613}{3.72*10^{-4}} = 1.65\,MPa \quad (28)$$

Axial strain and shortening:

$$\varepsilon = \frac{\sigma}{E_{fg}}, \quad \delta = \varepsilon L = \frac{F_{max} L}{A_c E_{fg}} \tag{29}$$

Using L=1.27 m and a representative placeholder $E_{fg} = 25\ GPa$:

$$\varepsilon = 6.6 * 10^{-5}, \ \delta = 8.4 * 10^{-5}\, m = 0.084\, mm \tag{30}$$

Check for buckling.
Second moment of inertia:

$$I = \frac{\pi}{64}(D_o^4 - D_i^4) = 2.81 * 10^{-7}\, m^4 \tag{31}$$

Euler critical load (conservative, K=1)

$$P_{cr} = \frac{\pi^2 E_{fg} I}{(KL)^2} \approx 4.3 * 10^4\, N \tag{32}$$

The fiberglass tube's area yields an axial compressive stress of 1.65 MPa at a max force of 613 N, which indicates that the airframe is not stress-limited. Using an approximated Young's modulus of E for fiberglass, predicted axial shortening is 0.084 mm; elastic deformation for ascent is negligible. Checking for Euler buckling using conservative values yields 43kN ≫613 N, so global buckling is also not a limiting factor for ascent. With this, our updated choice of fiberglass tubing proves sufficient for axial forces during flight.

Normal Force and Bending During Flight - Emilio Huggins

Using the same geometry above with a thrust load of 613 N and axial stress 1.65 MPa, assumptions were made to find the bending and combined stress to check the integrity of the fiberglass tubing.

- Air density at the launch site ($\approx 2600\ ft$): $1.14\ kg/m^3$
- AoA: $\alpha = 8.6^\circ = 0.150\ rad$
- $C_N = C_{N\alpha}\alpha = 0.901$
- Absolute max velocity: $V = 374\ m/s$
- Gust misalignment factor: $1.5 \times F_N$
- Body reference area (Outer Diameter): $S_{ref} = \pi D_o^2/4 = 0.00493\, m^3$
- Moment about rocket CG (Rocksim): $\Delta x = 14.509\ in = 0.3685\ m$

Dynamic pressure and normal forces:

$$q = \frac{1}{2}\rho V^2 = \frac{1}{2}(1.14)(365.46^2) = 7.61 * 10^4\, Pa \tag{33}$$

$$F_N = q\, S_{ref}\, C_N = (7.61 * 10^4)(0.00493)(0.901) = 3.38 * 10^2\, N \tag{34}$$

$$F_{N,des} = 1.5 F_N = 5.07 * 10^2 \tag{35}$$

Bending Moment / Stress about CG:

$$M \approx F_{N,des}\Delta x = (507)(0.3685) = 1.86 * 10^{2}\, N \bullet m \quad (36)$$

$$\sigma_b = \frac{Mc}{I} = \frac{(186)(0.03962)}{2.81*10^{-7}} = 2.62 * 10^{7}\, Pa = 26.2\, MPa \quad (37)$$

Combined stresses (axial and bending)

$$\sigma_{max} = \sigma_{ax} + \sigma_b = 1.65 + 26.2 = 27.85 \quad (38)$$

$$\sigma_{min} = \sigma_{az} - \sigma_b = 1.65 - 26.2 = -24.55 \quad (39)$$

When using a conservative bending estimate, the design normal force is 507 N. With rocksim CG spacing, this yields a moment M = 186 N · m and a bending stress of 26.2 MPa. The results of the combined max and min stresses indicate that flight loading is more bending-dominated than thrust compression.

Based on these combined stresses, the fiberglass G12-class airframe is structurally sound. Factor of safety (estimating from vendor details) can be calculated with a conservative allowable stress of 150-200 MPa as 5.0-6.5 against the $\sigma_{max} = 27.85$ MPa.

When compared to our initial choice of 3D printed PLA filament, our idealized FOS would be roughly 2, ignoring possible print defects and effects from heat.
Overall, our choice of fiberglass tubing allows for a much larger and more reliable margin and reduces the risk of failure due to manufacturing variables.

Motor Centering Ring Structural Analysis - Emilio Huggins

The analysis focuses on the physical properties and stress/strain susceptibility of the internal motor centering ring. The centering ring is charged with the responsibility of keeping the motor centered and preventing dislocation, ensuring stability during burn. Analysis was conducted considering the use of three different materials of the specified part, specifically Polylactic Acid (PLA), 6061-T6 Aluminum, and fiberglass laminate. For each material, the average compressive stress, strain, and factor of safety were calculated to justify the use of each material.

Assumptions and Variables

The stress analysis of the motor centering ring assumes a static peak thrust of 613 N from the H100 motor applied as a uniform pressure over the annular area between the 1.57 in inner bore and the 3.00 in outer diameter, neglecting the small area removed by slots and fastener holes and ignoring dynamic effects such as vibration, thrust oscillations, and landing loads. PLA, 6061-T6 aluminum, and fiberglass are each modeled as homogeneous, linearly elastic materials described by a single Young's modulus and yield (or design) strength at room temperature, and the attachment between the ring and the airframe is assumed to be stronger than the ring, so that only the ring is evaluated for failure. Under these assumptions, static

compressive strength is not the limiting factor, and the main design considerations become temperature tolerance near the motor, long-term stiffness and durability over multiple flights, manufacturability with available fabrication methods (3D printing, machining, or composite cutting), and compatibility with the surrounding aft structure. These simplifying assumptions provide a clear, conservative framework for verifying that the current centering-ring geometry can safely transfer thrust loads to the airframe while guiding material selection for the final flight hardware.

Modeling and Schematics

Figure 15 below provides the physical dimensions of the motor centering ring in inches.

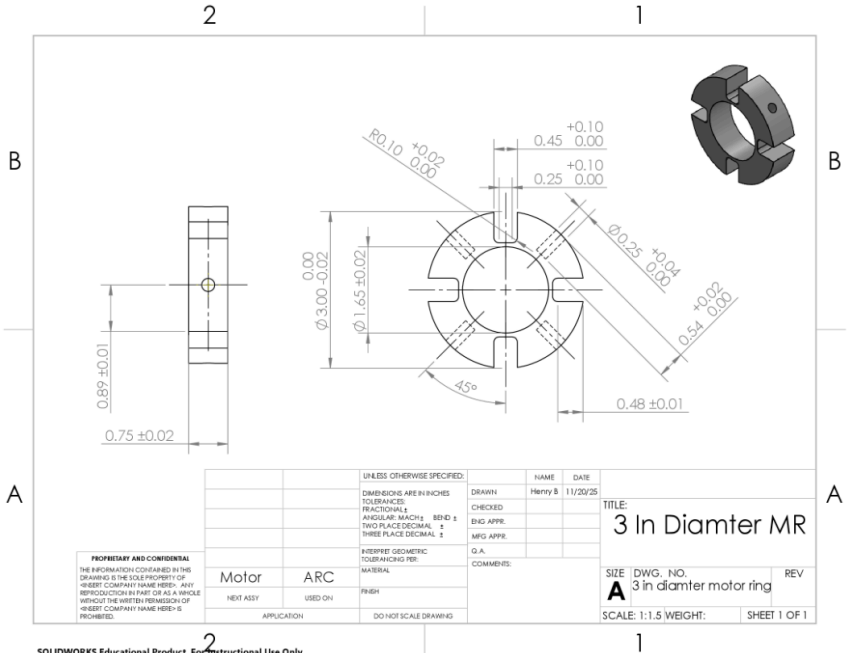

Figure 15: Motor Centering Ring

Calculations

The motor centering ring is modeled as a circular annulus that carries the axial thrust load from the solid rocket motor into the airframe. The design load is taken as the motor's maximum thrust, $F = 613N \approx 138\,lbf$, applied uniformly over the annular face between the inner diameter $D_i = 1.57\,in$ (motor mount bore) and outer diameter $D_o = 3.00\,in$ (outer edge of the ring). Under this idealization, the load-bearing area is the full annular area,

$$A = \frac{\pi}{4}(D_o^2 - D_i^2) \tag{40}$$

and the average compressive stress in the ring is

$$\sigma = \frac{F}{A} \tag{41}$$

Each candidate material—3D-printed PLA, 6061-T6 aluminum, and fiberglass—is treated as homogeneous and linearly elastic in the loading direction, characterized by a Young's modulus E and a room-temperature yield (or design) strength σ_y. The corresponding elastic strain is calculated from

$$\varepsilon = \frac{\sigma}{E}, \tag{42}$$

and the factor of safety with respect to yielding is defined as

$$N = \frac{\sigma_y}{\sigma} \tag{43}$$

A sensitivity check is also performed by repeating the stress and factor-of-safety calculations with a reduced effective area (0.69 in²) to represent the case where only a subset of the ring cross-section carries most of the thrust. Together, these relations provide a simple analytical model that links the applied thrust, ring geometry, and material properties to the key performance metrics of stress, strain, and factor of safety.

Results and Discussion

Using the full annular area between 1.57 in and 3.00 in, the average compressive stress in the centering ring under the 613 N design load is on the order of 27 psi, which is extremely small compared with typical yield strengths for PLA, aluminum, and fiberglass. The corresponding elastic strains are on the order of $10^{-6} – 10^{-5}$, indicating that the ring will experience negligible compression and will maintain motor alignment with the airframe during boost. Even when the effective area is reduced to 0.69 in² to represent a worst-case load path through the inner webs, the stress rises only to about 200 psi, and the resulting factors of safety remain very large—on the order of tens for PLA and hundreds for aluminum and fiberglass. These results show that, under the assumed loading, static compressive strength is not the limiting design constraint for the centering ring in any of the three materials. Instead, material choice should be driven by secondary considerations such as temperature tolerance near the motor, stiffness, and long-term dimensional stability, manufacturability with available processes (3D printing, machining, or composite cutting), and integration with surrounding structures. From this perspective, PLA is desirable for rapid prototyping and low-temperature use, while aluminum and fiberglass offer greater thermal robustness and long-term durability for flight hardware, all while easily satisfying the basic strength requirements predicted by the analytical model.

Material	E (PSI)	σ (PSI)	σ_y (PSI)	ε	N
PLA (3D Printed)	$4.35 * 10^5$	7250	26.9	$6.2 * 10^{-5}$	270
6060-T6 Aluminum	$1.00 * 10^7$	40000	26.9	$2.7 * 10^{-6}$	1490
Fiberglass	$1.04 * 10^7$	71000	26.9	$2.6 * 10^{-6}$	2640

Table 7: Centering Ring Results

Control Mechanism and Force - Chyler Bitsoi

This section outlines the analysis baseline upon which the active fin actuation system for the ARC rocket was confirmed to be feasible and structurally sound. Two governing conditions of operation were

analyzed: (1) the roll acceleration required to intentionally generate a commanded roll rate of ±100 RPM and (2) the servo-actuated linkage geometry generating maximum mechanical loading at the most adverse aerodynamic condition before maximum dynamic pressure.

These governing conditions represent the extremes of operation for the actuation system and facilitate servo and pushrod material selection.

Required Roll Moment for active control (Roll Acceleration Case)

To effectively command and suppress a commanded roll, the necessary control system torque must surpass the rocket's inertia of motion for roll acceleration and roll deceleration. The required roll moment was determined with respect to.

$$M_{req} = I_z \alpha \tag{44}$$

Where I_z is the mass moment of inertia about the z-axis of the rocket, and α is the angular acceleration that will achieve the commanded roll rate. The commanded roll rate of 100 RPM was converted to radians/sec and determined as a relative value of the effective required roll moment to condition control. These conditions place a control authority requirement as a function of the minimum available authority of the fin system.

Aerodynamic Fin Loading and Hinge Moment (Maximum Dynamic Pressure Case)

The aerodynamic loading on the aft fins corresponds to the maximum ascent velocity determined by RockSim; this is where dynamic pressure reaches a peak value during ascent. Thus, this is the largest threat to aerodynamic loading on control surfaces.

The maximum predicted velocity is 1150 ft/s, and thus, the fin normal force and resulting hinge moment are proportional to dynamic pressure. As hinge moment increases exponentially with velocity, determining it as a derivative of this worst-case scenario is enough to show that the aerodynamic hinge moment is, at this worst-case scenario, still less than the stall torque rendering of the selected servo. Therefore, it is not aerodynamic loading that controls the maximum transfer of force through the actuation drive system.

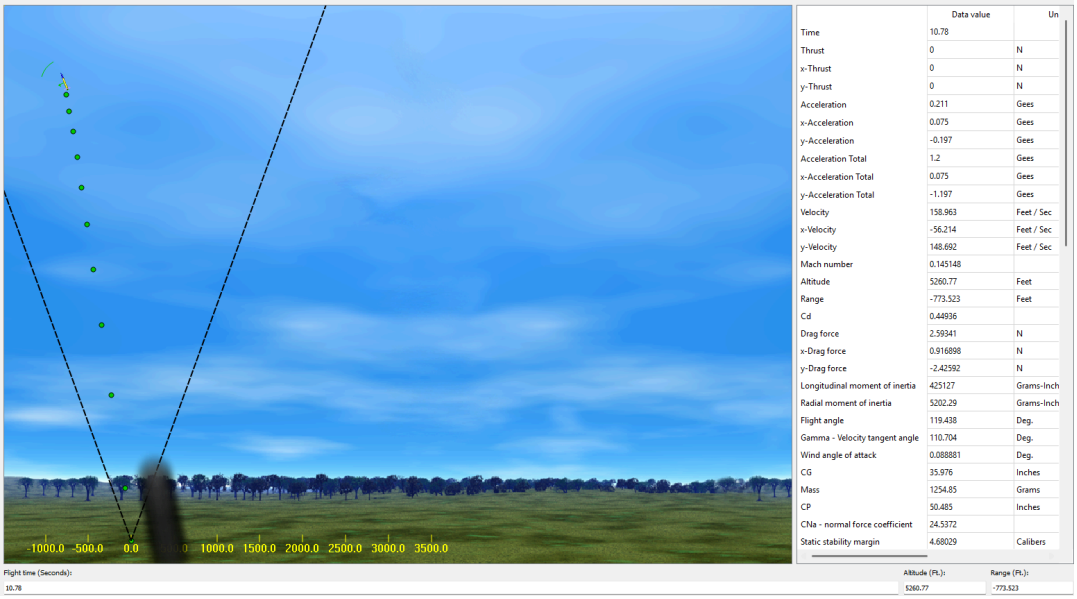

Figure 16: Rocksim Data

Servo Torque Limitation and Pushrod Force (Servo-Limited Case)

Because aerodynamic hinge moments are not greater than actuator ability, the working internal load condition is determined to be the servo stall torque. For the KST X15-755X chosen, the stall torque is rated at 8.85 lbf·in, which is the highest mechanical load that transfers through the linkage in either direction without concern for the contribution of hinge moment dynamics.

Using the servo stall torque and horn geometry, it was determined that the pushrod force would be nominally between 17 and 22 lbf. This servo-limited condition governs all subsequent structural analysis of the pushrod and joint hardware.

Pushrod Structural Evaluation (Stability-Governing Case)

The push rod was tested for the servo-limited force. A preliminary look at axial stress indicates that neither candidate material fails strength requirements. However, with pin boundary conditions and its slender geometry, compressive stability will govern performance.

For instance, Euler buckling calculations show the critical buckling load of 6061-T6 aluminum to be much greater than the governing servo-limited force; PLA does not meet the same requirement. Therefore, stability of the push rod—over axial stress—will govern material selection.

Engineering Calculation Equation Summary:

The equations below are the governing relationships used to evaluate the active fin actuation mechanism for the chosen load cases. They were used based on RockSim flight conditions and CAD model geometry dimensions. A deeper dive into the derivation and steps in between can be found in the Advanced Analysis Homework and the appendices referenced.

Roll Dynamics (Roll Acceleration Case):

Used to determine the minimum roll moment required to induce the required 100 RPM roll rate.

$$M_{req} = I_z a \tag{44}$$

$$a = w/t \tag{45}$$

$$w = 100\ RPM \tag{46}$$

Used to estimate the fin normal force and hinge moment at peak ascent velocity

$$q = \frac{1}{2}\rho V^2 \tag{47}$$

$$L = qSC_l \tag{48}$$

$$M_h = Lx_{cp} \tag{49}$$

Used to determine the maximum internal force transmitted through the control linkage.

$$F_{rod,max} = \frac{T_{stall}}{r_s} \tag{50}$$

Used to verify material strength under maximum servo-limited loading.

$$\sigma = \frac{F}{A} \tag{51}$$

Used to assess the compressive stability of the slender pushrod and its material.

$$P_{cr} = \frac{\pi^2 EI}{(KL)^2} \tag{52}$$

$$I = \frac{\pi d^4}{64} \tag{53}$$

Used to confirm that joint hardware does not govern failure.

$$\tau = \frac{F}{2A_p} \tag{54}$$

Section Summary and Governing Results:

Results from the analyses performed in this section validate that the active fin actuation mechanism is mechanically feasible and structurally sound when subject to the expected loading conditions of the flight environment. Required roll moments analyses define the lower limit of control authority needed to generate and cancel a 100 RPM roll rate, since the aerodynamic fin system can at least do this much. Furthermore, fin aerodynamic loading analysis at the maximum dynamic pressure condition indicates effective actuator torque by the selected servos.

Thus, the governing internal loading conditions for the actuation mechanism are limited by the actuator itself, not included in the aerodynamic loading. The KST X15-755x stall torque represents the greatest amount of applied force (through the linkage) that may occur, meaning that a resultant force from the

pushrod is expected to be within the range of 17 lbf to 22lbf based on the effective geometry of the horn. Pushrod structural analysis indicates that normal stress due to axial loading is safely below material strength for both materials; however, geometry and pinned boundary conditions will make stability, as determined by compressive strength performance, more critical for the determination of feasibility. Thus, Euler buckling analysis suggests that 6061 T6 Aluminum provides a safety factor against buckling due to loads by the servo while PLA fails to do so, with a specified safety range.

Thus, these results support the KST X15-755x servo and aluminum pushrod for the active fin, which are integral to flight, and confirm that sufficient roll control can be achieved without compromising pushrod stability during all the intended flight environments.

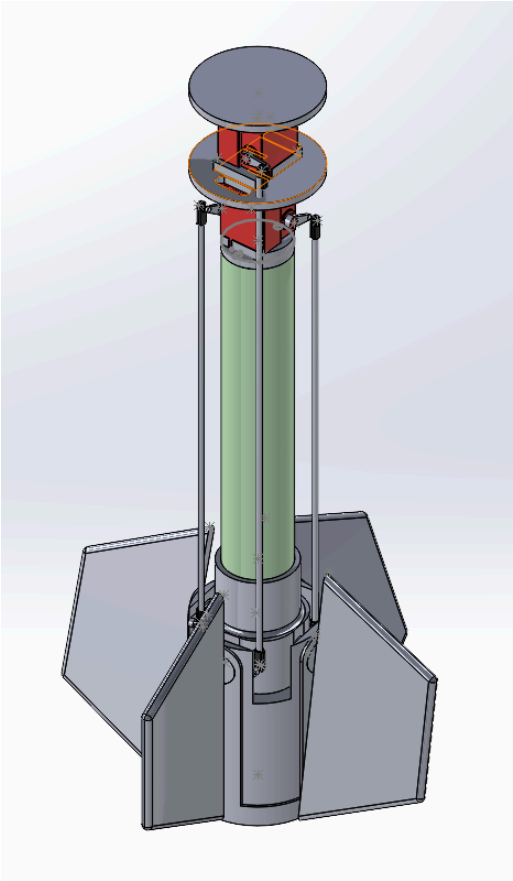

Figure 17: Aft Control mechanism

Factor of Safety Table:

Sub System	Part	Load Scenario	Material	Method of calculating FoS	Minimum FoS
Motor Housing					
	Airframe	Peak thrust $F_{max} = 613\ N$ + conservative bending (AoA= 8.6°, gust factor = 1.5) $\sigma_{max} = 27.85\ MPa$	G12 Fiberglass tube	Hand Calculations	5.4
	Screws	$1280\ N$	A574 Alloy Steel	Hand Calculations and FEA	2
	Motor Rings	Axial Load 613 N (Worst Case reduced print area)	PLA	Hand Calculations	200
Control System					
	Servo Output (Torque)	Maximum roll and stall torque	Aluminum	Hand Calculations using stall torque vs required hinge moment	1.5
	Pushrod (Axial Stress)	Servo-Limited push rod force (17-22lbf)	Aluminum 6061-T6	Hand Calculations	20
	Pushrod (Buckling Force)	Servo-limited compressive force, pinned–pinned column	Aluminum 6061-T6	Hand Calculation - Euler buckling analysis	2
	Pushrod (Buckling Force)	Servo-limited compressive force, pinned–pinned column	PLA	Hand Calculation - Euler buckling analysis	1.0 (Failed)
	Clevis / Pin Joint	Servo-limited force in double shear	Steel pin	Hand calculations	5
	AoA of Fins	$200\ m/s\ and\ at\ 3000ft$	N/A	Hand Calculations	1

Table 8: Factor of Safety by Subsystem

Flow Chart - Eric Reyes:

Subsystems Flow Chart

The following flowchart summarizes how each subsystem contributes to the launch sequence, with a heavier emphasis on the final outcome (launch).

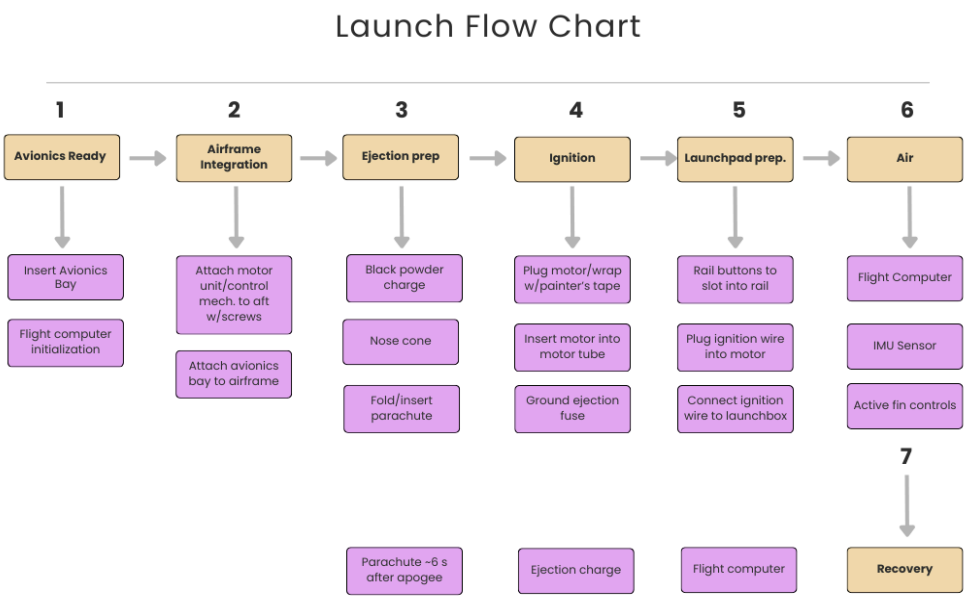

Figure 18: Launch Flow Chart

As can be seen in the launch flow chart, several external components are required that are not part of the ARC vehicle itself, including the ejection fuse, ignition wiring, and launch box. While these elements are standard for solid-rocket launches, they are only involved during the ground-controlled ignition phase of the first launch. In contrast, onboard components such as the flight computer and active fin system remain integral to the vehicle and become functionally active during the hangtime of flight.

Flight Computer Sequence Flow Chart

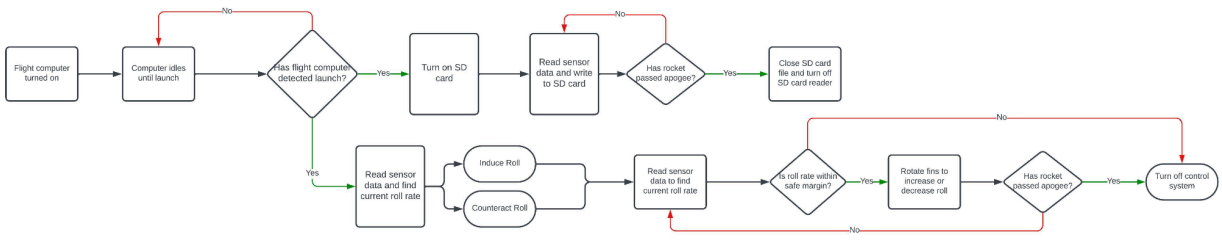

Figure 19: Flight Computer Sequence Flow Chart

Above is the Flight Computer Sequence Flow Chart. This subsystem is based on an Arduino circuit that is driven by an SD card reader for read/write data from an IMU that provides gyroscopic sensor data. As shown, these two components work in synergy to detect launch, read/write sensor data, and use the data to make decisions such as *induce* or *counteract* roll in the active fins subsystem.

Moving forward:

This report presents an up-to-date, comprehensive set of preliminary calculations and analyses supporting the feasibility of the Active Rocket Control (ARC) system. Specifically, the report evaluated fastener shear strength for the motor retention system, fin aerodynamic behavior and control authority for roll induction and suppression, ejection charge sizing and parachute recovery requirements, axial and bending stresses in the fiberglass fuselage, and compressive loading of the motor centering ring for material selection. Subsystem factors of safety were also set.

With these items completed, that leaves room for some areas to improve on. For instance, the active fin subsystem needs to be explored, developing a time domain test with our Electrical Engineering Team. This ensures the timing of automatic adjustments made to the active fins is properly responsive to the environment. Continuing with active fin development, a kinematic analysis of the fin actuation is another necessary step to confirm deflection angles, motion limits, and mechanical response under dynamic loading. While we have the fin angle now, it is subject to change as the assembly of our rocket changes in mass property distribution. Continuing to perform RockSim analyses, despite the current ones presented being the most up-to-date, is crucial as we adjust the assembly of the rocket. Mass properties of the internal layout are yet to be finalized, so it is crucial to uphold this practice of performing RockSim analyses.

While the current evaluations, the active fin actuation concept is mechanically feasible and generates adequate roll control forces, future efforts to further reduce technical risk and increase confidence in the final design will include CFD on the fully assembled vehicle—CFD will provide better insight into realistic flow around the aft body and control fins, as current aerodynamic considerations are over-simplified to provide basic input for aerodynamic loading, potential flow separation, and asymmetric forces. CFD will either support or deny hinge moment expectations based on conservatively assumed findings in previous design assessments.

Simultaneously, as the bearing loads at the aft mechanism of control were ignored for evaluation, future mechanical considerations will be more comprehensive from the perspective of the fin shaft and potential bearing interactions. A rotating shaft will impose bearing loads, friction considerations, and wear possibilities that have not been sufficiently explored. Kinematic force analysis of a comprehensive shaft-bearings interface will be completed with more precise part geometry to represent internal loading, joint forces, and alignment complicating factors. Addressing these considerations will ensure that active fin actuation continues to be reliable and robust through realistic loading throughout the full range of anticipated flight conditions.

Lastly, standards and codes need to be explored further to ensure our approach is credible. Specifically, Tripoli safety codes are an external standard that needs to be followed more to ensure that we comply with all regulations and rocket standards in order to participate in the launch. In designing, engineering requirements from our advisor, Professor Pete, were components we were more cognizant of. Still, we need to double-check adherence to engineering requirements. For instance, components are changing in material or are off the shelf, and at least 50% of components need to be custom-fabricated. Nuances like this in the customer/engineering requirements need to be revisited as it is easy to overlook them.

References

[1] “Tripoli Rocketry Association Safety Code ,” unified safety code - Tripoli Rocketry Association, https://www.tripoli.org/safetycode#:~:text=A%20rocket%20shall%20be%20launched,12%2D5.1 (accessed Nov. 22, 2025).

[2] I. Apogee Components, “Apogee components - Aerotech 38mm HP SU DMS motor - I500T-14A,” I500 Blue Thunder Disposable Motor System, https://www.apogeerockets.com/Rocket_Motors/AeroTech_Motors/38mm_Motors_Single_Use/Aerotech_38mm_Motor_I500T-14A_HP_SU (accessed Nov. 20, 2025)

[3] R. G. Budynas and J. K. Nisbett, Shigley’s Mechanical Engineering Design, 8th ed. New York, NY, USA: McGraw-Hill, 2008 (accessed Nov. 20, 2025).

[4] “Free CAD designs, Files & 3D models: The grabcad community library,” Free CAD Designs, Files & 3D Models | The GrabCAD Community Library, https://grabcad.com/library/screw-1-4-1 (accessed Nov. 20, 2025).

[5] Polylactic acid (PLA) filament for 3D printing:Uses & Applications, https://www.divbyz.com/knowledge-center/materials/pla (accessed Nov. 20, 2025).

[6] “G12 fiberglass filament wound tube,” frp insulation material factory, https://www.frpinsulation.com/index.php/2020/08/27/g12-fiberglass-filament-wound-tube/(accessed Nov. 20, 2025).

[7] “1/4-20 x 4 A574 alloy steel socket head Cap Screw,” STS Industrial, https://www.stsindustrial.com/products/0-25-20x4-alloy-steel-socket-head-cap-screw/?head_type=Socket#:~:text=Chemical%20PropertiesAlloy%20Steel%20Socket%20Head%20Cap%20Screw&text=1.,(55%20%C3%97%20carbon%20content). (accessed Nov. 21, 2025).

[8] R. Nakka, “Introduction to Rocket Design: Fins,” Richard Nakka’s Experimental Rocketry Site, https://www.nakka-rocketry.net/RD_fin.htm (accessed Dec. 23, 2025).

[9] J. Barrowman, “James S. Barrowman (#6883) Judith A. ...,” The Practical Calculations of the Aerodynamic Characteristics of Slender Finned Vehicles , https://www.nakka-rocketry.net/articles/Barrowman.NARAM-8.pdf (accessed Jan. 22, 2026).

[10] “Area of trapezoid - formula: How to find the area of a trapezoid?,” Cuemath, https://www.cuemath.com/measurement/area-of-trapezoid/ (accessed Jan. 23, 2026).

[11] Admin, “Moment of inertia of a hollow cylinder,” BYJUS, https://byjus.com/jee/moment-of-inertia-of-a-hollow-cylinder/?utm_source (accessed Jan. 23, 2026).

[12] Admin, “Moment of inertia of cone,” BYJUS, https://byjus.com/jee/moment-of-inertia-of-a-cone/ (accessed Jan. 23, 2026).

[13] Alechner, “Refresher on the basics of angular acceleration and moment of inertia,” R+W Coupling Technology,https://www.rw-america.com/refresher-on-the-basics-of-angular-acceleration-and-moment-of-inertia/ (accessed Jan. 23, 2026)

[14] I. Apogee Components, “Advanced construction videos : Apogee rockets, model rocketry excitement starts here,” Advanced Construction Videos : Apogee Rockets, Model Rocketry Excitement Starts Here, https://www.apogeerockets.com/Advanced_Construction_Videos/Rocketry_Video_337 (accessed Nov. 22, 2025).

[15] “Black powder sizing,” Info Central, https://info-central.rocketlabdelta.com/recovery/black-powder sizing/#:~:text=This%20is%20the%20simplest%20case%20for%20a,in/ft%20to%20get%20in%20terms%20of%20inches.) (accessed Nov. 22, 2025).

[16] Wickenburg, AZ hourly weather forecaststar_ratehome. Weather Underground. (n.d.).https://www.wunderground.com/hourly/us/az/wickenburg

[17] Apogeerockets, https://www.apogeerockets.com/downloads/PDFs/Peak-of-Flight-Newsletter-Rocket Plans.pdf (accessed Nov. 23, 2025).

[18] I. Apogee Components, “Apogee components - Aerotech 38mm HP SU DMS motor - H100W-14A,” [81295] - $58.84 : Apogee Rockets, Model Rocketry Excitement Starts Here, https://www.apogeerockets.com/Rocket-Motors/AeroTech-Motors/38mm-Motors-Single Use/Aerotech-38mm-HP-SU-Motor-H100W-14A#faqs (accessed Nov. 22, 2025).

[19] Embry-Riddle Aeronautical University, “Worked Examples: Bluff Body Flows,” Introduction to Aerospace Flight Vehicles. Accessed: Jan. 25, 2026

[20] Madcow Rocketry, “3" G12 Airframe,” Madcow Rocketry. Accessed: Dec 22 2025

[21] https://www.homedepot.com/p/Prime-Line-1-4-in-20-x-1-1-4-in-Black-Oxide-Coated-Steel-Hex-Allen-Drive-Socket-Head-Cap-Screws-10-Pack-9178581/311491926?MERCH=REC-_-rv_nav_plp_rr-_-n%2Fa-_-2-_-n%2Fa-_-n%2Fa-_-n%2Fa-_-n%2Fa-_-n%2Fa (accessed Nov. 21,2025).